NO_2 Chemiluminescent Emission from Flames Influenced by Acoustic Noise

Ki Yong Lee* and Ishwar K. Puri**

(Received August 28, 1997)

The effect of acoustic noise on combustion is investigated from the perspective of NO_x emissions. A robust, plug-in probe that exploits the natural emission signal from the combustion gases, and which can have practical relevance, is used. Acoustically pulsed flames are stabilized on a burner, and NO_2 chemiluminescence is measured with an intensified detector at various frequencies. The results indicate the NO_2 emission increases in noisy flames at certain frequencies more significantly than others. Noise at higher frequencies in the range 0.8~1 kHz effects the nitrogen chemistry in stoichiometric flames ($\phi=1$), but not that in lean flames ($\phi=$ 0.7 and 0.8).

Key Words: NO_2, Chemiluminescence, Emission, Flat Flame, Acoustic Noise, Burner

1. Introduction

Acoustic noise have an important influence on the premixed combustion, and produce the large-amplitude pressure fluctuations which, when coupled with oscillations in the heat release, can decrease system performance efficiencies. On the other hand, judicious use of combustion oscillations can increase the chemical heat release rate, and reduce the emission of pollutants (McManus et al., 1993). However, acoustic noise (particularly, that at higher frequencies) can be an environmental nuisance in practical devices, and little is known of its effect on NO_x formation. The objective of this research is to investigate the effect of noise on NO_x emissions with a device that has practical relevance. For this reason, a robust, plug-in probe that exploits the natural emission signal from the combustion gases is developed.

* Andong National University Department of Mechanical Engineering 388 Songchun-Dong Andong, Kyungbuk 760-749

** University of Illinois at Chicago Department of Mechanical Engineering (M/C 251) Chicago, Illinois 60607-7022

2. Methodology

We have measured NO_2 chemiluminescent emission from CH_4/Air premixed flames that have acoustic noise imposed on them. The imposition of noise simulates geometries in which it would be naturally produced. The flames at various equivalence ratios, i. e., $\phi=0.7$, 0.8, and 1.0, are established using a premixed flat flame burner. A loudspeaker is used to produce the acoustic waves in the higher frequency range of 800~18000 Hz. This range which is different from the natural frequency range of the flame is deliberately chosen to investigate the effect of higher frequency noise, and to avoid pressure-thermochemical resonance. In our experiments, the acoustic energy supplied to the flames is negligibly small compared with their thermochemical heat release. Chemiluminescent emission from NO_2 is investigated at 840 nm (Pearse and Gaydon, 1976, Clyne et al., 1964) using an intensified imaging system.

A schematic diagram of the flat flame burner is presented in Fig. 1. The stainless steel burner is surrounded by a coannular outer duct that provides a uniform curtain flow of nitrogen to isolate the flames from ambient disturbances. A steel

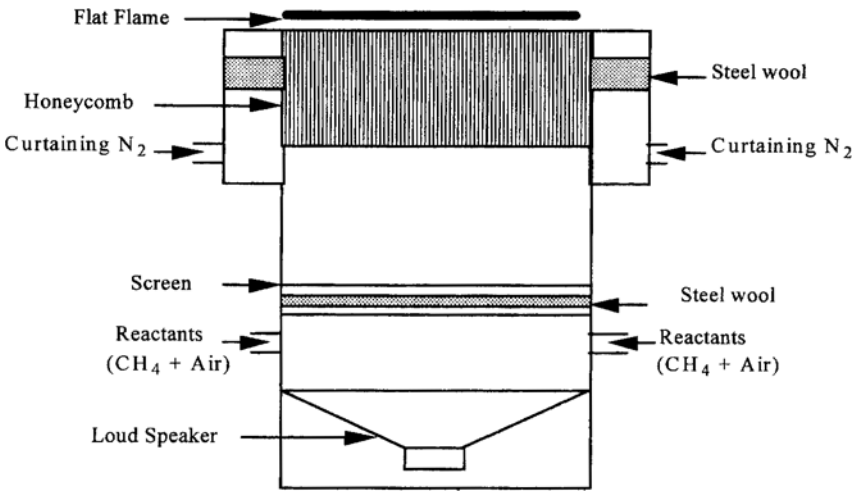

Fig. 1 Schematic diagram of the flat flame burner assembly.

Table 1 Velocities and flowrates during the experiments of reactants with respect to equivalence ratio. Predictions for corresponding freely propagating flames are presented in parentheses.

ϕ	CH_4 ($cm^3\ sec^{-1}$)	Air ($cm^3\ sec^{-1}$)	Velocity ($cm\ sec^{-1}$)
0.7	60.42	822.08	24.3(21.4)
0.8	87.24	1038.58	31.0(30.6)
1.0	125.61	1196.32	36.4(40.8)

wool and stainless steel screen arrangement are placed inside the inner duct following the reactant inlets to induce the laminar flow, following which the reactants pass through a ceramic honeycomb (EX20 Cordierite, Corning Glass) having a density of 62 cells cm^{-2}, and exit under uniform laminar conditions at the burner surface. The diameter of the surface on which the flames are established is 68 mm. The static pressure loading on the speaker is carefully eliminated.

Methane (commercial grade, 93% pure from natural gas) is used as fuel, commercial grade nitrogen for the curtaining flow, and shop air as oxidizer, all of which are supplied through the calibrated flowmeters. The flame speed of methane is converted into the reactant flowrates (or velocities) as shown in Table 1.

Predictions of the corresponding propagating flames are made using the set of Sandia codes (Kee et al., 1989 and Kee et al., 1985) with well-characterized methane-air (Frenklach et al., 1994) and nitrogen (Miller and Bowman, 1989) chemical kinetic mechanisms. The computer code requires inputs for the molecular and thermodynamic properties of the species that are part of the reacting system in a standard format (Kee et al., 1989). The predicted freely propagating flame speeds for the corresponding set of flames are reported in Table 1.

The acoustic generating system consists of a speaker (Radio Shack, 76 mm dia. midrange/tweeter speaker, 30 W maximum power), a cross-over capacitor, an amplifier (Radio Shack, 35 W), and a function generator. The function generator produces a sine waveform attenuated at 0 dB, and the frequencies 0.8, 1, 2, 5, 10, 15, and 18 kHz are employed in the experiments. In order to determine and establish the frequency response curve, there is negligible absorption of acoustic energy inside the burner, loudspeaker sound levels are measured with and without the burner duct enclosing the speaker. With constant speaker input voltage of 14V(RMS), results for an A-weighted sound meter response are presented in Fig. 2. We note that in our experiments frequencies with similar loudness can be divided into three sets. The first set consists of frequencies

between 0.8~1k Hz, the loudness of which is about 108 dB, the second in the range 2~10 kHz, the loudness of which is about 114 dB, with the third set containing frequencies over 10 kHz at which the sound level rapidly decreases. The results show no dissipation of energy due to the burner duct and honeycomb.

A schematic diagram of the imaging system is presented in Fig. 3. It consists of a convex lens, a monochromator (1/8 m, Oriel Corp.), and an intensified CCD camera (F4577, ITT). The radiant flux increases as the inverse of the square of the F No. (=f/D, where f denotes the lens focal length and D the diameter of the first convex lens). For our system D and f are 50 mm and 100 mm respectively. The second lens is planoconvex of D=25.4 mm and f=38.1 mm. The resolution of the monochromator is 0.5 nm for a grating corresponding to 1200 lines/mm and a 50 mm slit.

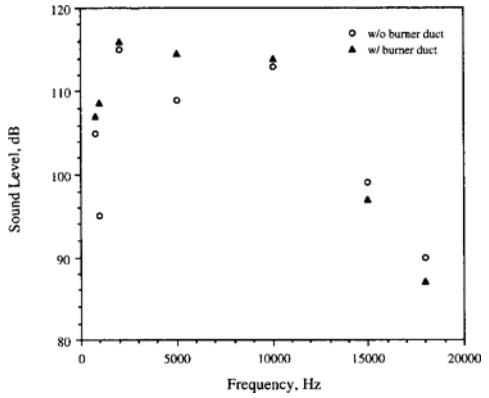

Fig. 2 The measured sound level of acoustic waves with respect to frequencies from the speaker with and without the burner duct.

In the experiments the entrance and the exit slit widths are set at 0.2 mm which correspond to a bandpass of ±1.1 nm (at 0.5 of peak transmittance), and the slit height is maintained at 12 mm. The spectral response of the CCD camera is relatively flat in the range between 420~900 nm, and is 0.02 Amps/Watt at 840 nm.

The images from the CCD camera are transferred to a frame grabber (P360F, Dipix) in a PC, digitized and stored into a buffer by image acquisition and processing software (Accuware). It takes the grabber 1.045×10^{-6} sec to digitize the analog signals for a set of 30 images that are recorded during each experiment. From the entire set the four best flame and four background images are analyzed using a histogram analysis. The histogram of each image is written in a matrix that contains one number for each of the 256 possible gray levels which a pixel can have. This intensity represents a measurement of the emission of recorded by the detector. The total emission intensity is obtained by integrating the flame image pixel gray level matrix and subtracting the corresponding background image from it. Measurements of the background are made just prior to the experiments.

3. Results and Discussion

The chemiluminescent emission due to NO_2 is investigated at 840 nm (Pearse and Gaydon, 1976, Clyne et al., 1964). According to Pearse and Gaydon's book, ten emission bands are recommended to monitor NO_2 emission in the range 608.8~851.5 nm. We have investigated the flames

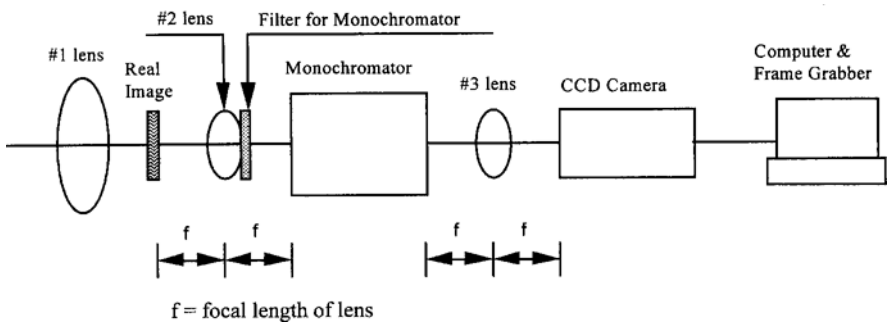

Fig. 3 Schematic diagram of the imaging system.

at $\phi=0.8$ to determine those bands that have been recorded more intensely by the imaging system. The intensity decreases in the order $\lambda=840$, 851.5, 753.3, and 802.4 nm. The recorded intensity at the remaining bands is low, and lies within the noise level of the imaging system. Three emission bands (791.9, 799, and 802.4 nm) around 800 nm overlap with H_2O emission and an OH chemiluminescence band occurs at $\lambda=752.15$ nm (Gaydon, 1974). Therefore, the wavelengths at 753.3 and 802.4 nm are discarded, and 840 nm is chosen to record the NO_2 chemiluminescence.

The "exposure time" to obtain a single image is 1/30 second. The number of waves passing through the flame during that time depends on the wave frequency. By generating acoustic waves at frequencies greater than 30 Hz, more than one wavelength pass through the flame during the time the signal is being recorded. Therefore, a single image contains intensities emitted from the various portion of the flame region that is affected by different amplitudes of the acoustic wave. The background emission occupies a significant fraction of the net integrated gray levels for weaker flames. For instance, the ratio of the integrated gray level from the flame alone to that is 0.14 for an undisturbed (0 Hz) flame at $\phi=0.7$ due to net emission from both the flame and the background. This ratio rises to 0.37 for a similar flame at $\phi=1$.

A Czerny-Turner monochromator was used to obtain the images. The monochromator consists of two concave mirrors and one plan diffraction grating. One mirror collimates an image or the light source of the entrance slit, and the other one focuses the dispersed image or light from the grating to the exit slit. Therefore, spherical aberration and astigmatism of the mirror remain at all wavelengths. In an ideal case all paraxial rays striking the mirror at some point are brought to a focal point. If, however, the light is not confined to a paraxial region, all rays from one object point do not come to a focus at a common point (the phenomena known as spherical aberration (Jenkins and White, 1976)). A defective image also occurs when an object point lies some distance from the axis of a concave mirror. In this case the incident rays, whether parallel or not, make an appreciable angle with the mirror axis. The result is that, instead of a point image, two mutually perpendicular line images or a circular disk are formed, i. e., if a screen is placed far away from the mirror and moved toward the mirror, the image becomes a vertical line, a circular disk, and a horizontal line (Jenkins and White, 1990).

The sharp images of the flame may be formed at any distance, since bundles of parallel rays close to the axis, and the rays angled slightly with it, are brought to a sharp focus in the focal plane. Astigmatism is the prime disadvantage of most grating mountings, since the spectrum line is blurred along the length of the flame. Therefore, we cannot investigate the variation of the spectrum with height in the flame (Gaydon, 1974). However, it is possible to compare the entire images of flames obtained at different conditions (i. e., varying equivalence ratios and frequencies).

The ratios of the reactant flow rate at $\phi=1$ to that at other equivalence ratios are presented in Table 2. For the flame at $\phi=0.8$, the decrease in the NO_2 emission intensity relative to a stoichiometric flame is proportional to the decrease in fuel flowrate, but for $\phi=0.7$ the decrease in intensity is lower than the corresponding decrease in fuel. Comparisons of the predicted postflame peak NO and NO_2 mole fractions relative to stoichiometric flames are also presented in Table

Table 2 Ratio of fuel flowrate and intensity for ϕ compared to $\phi=1.0$ at $\lambda=840$ nm. Predictions for corresponding freely propagating flames are presented in parentheses.

ϕ	0.7	0.8	1.0
$\frac{Q_{fuel,\phi}}{Q_{fuel,\phi=1}}$	0.48	0.69	1.0
$\frac{I_{840nm,\phi}}{I_{840nm,\phi=1}}$	0.28	0.70	1.0
$Peak\frac{NO_{2,\phi}}{NO_{2,\phi=1}}$	(0.24)	(0.70)	(1.0)
$Peak\ \frac{NO_\phi}{NO_{\phi=1}}$	(0.04)	(0.18)	(1.0)
$Peak\ \ Temp.$, K	(1838)	(2001)	(2231)

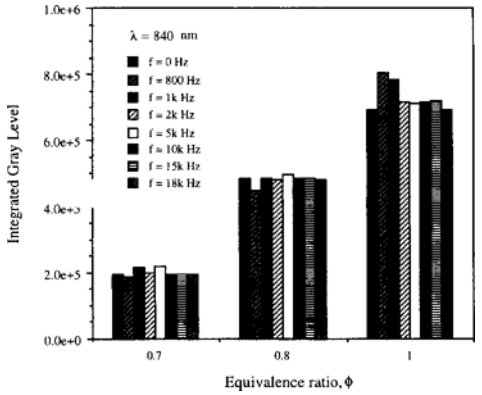

Fig. 4 Variation of the integrated gray level with respect to ϕ for $\lambda=840$ nm.

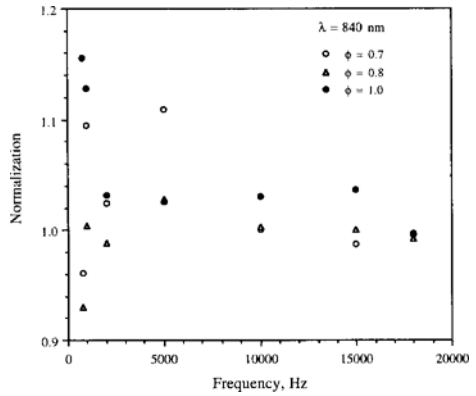

Fig. 5 The integrated gray level, normalized by 0 Hz signal, with respect to frequency for $\lambda=840$ nm.

2. The emission intensity relative to a stoichiometric flame shows good correlation with the relative postflame NO_2 at $\phi=0.8$ and a small incremental departure at $\phi=0.7$.

The variation in the integrated gray level with respect to the equivalence ratio is presented in Fig. 4. As the equivalence ratio increases, so does the integrated gray level. The integrated gray levels of acoustically influenced flames are divided by the integrated level corresponding to an undisturbed (0 Hz) flame, results for which are shown in Fig. 5. The low frequency data lie within the limits of experimental uncertainty for flames at $\phi=0.7$ and 0.8. Although, the flame at $\phi=0.7$ shows a small variation in the emission intensities with acoustic disturbance, this variation lies within the limits of experimental uncertainty. The stoichiometric flames, however, are significantly influenced by lower frequency waves, as illustrated in Fig. 4 and 5 with NO_2 levels that are 15% higher than the corresponding acoustically undisturbed flames. We observe that while lean flames are relatively unaffected by acoustic noise, the stoichiometric flames respond up to frequencies of 1 kHz. Small variations in the speaker sound level do not influence the emission from the noise -influenced flames. These results are consistent with the conclusion of Schimmer and Vortmeyer that the flame stability is a function of the frequency and the equivalence ratio. That investigation determined that only inductive acoustic oscillations with the frequency less than about 833 Hz were able to influence stoichiometric propane-air flames.

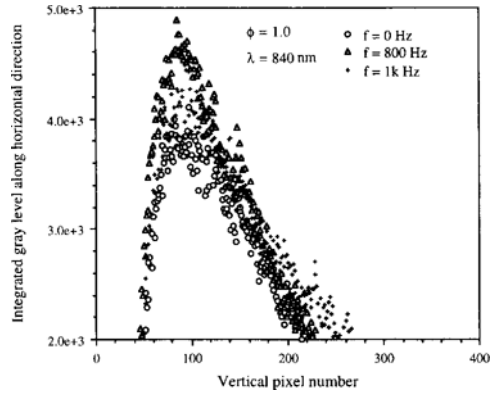

Fig. 6 The integrated gray level along the horizontal direction with respect to the vertical pixel number in an averaged image at different frequencies.

In Fig. 6 the variation of the integrated gray level along the axial direction is presented for $\phi=1$ flames established at 0.8 and 1 kHz. Due to the effect of noise, the integrated gray level at f=800 Hz is larger (by about 25%) than that for an undisturbed flame. Upon increasing the frequency from 0.8 to 1 kHz, the integrated gray level in the flame zone decreases implying the smaller effect on NO_2 emission. This indicates that the nitrogen chemistry is considerably suppressed in the leaner flames due to both thermal and chemical effects. The acoustic disturbances have their strongest effect on the flames with the more robust nitrogen

chemistry. In the flame at $\phi=1$ the chemical time scale associated with the nitrogen chemistry is much smaller than that in the flames at $\phi=0.7$ and 0.8, and is of order of 3 ms (Lentini and Puri, 1997). Therefore, frequencies around 1 kHz have more significant effects on the stoichiometric flames. In contrast, the chemical time scale associated with NO_x formation increases considerably in the leaner flames so that much smaller frequencies than those were investigated are anticipated to influence those flames.

4. Conclusions

The effect of acoustic noise on NO_2 chemiluminescence intensity was investigated in premixed flames with a robust and "practical" probe.

(1) The emission measurements were validated by comparison with predictions that used well characterized chemistry. The measurements correlate well with the postflame NO_2 maxima for flames at $\phi=0.8$ and 1.0.

(2) The experiments concur with the previous investigation of the noise effect on flame stability.

(3) For small variations, the speaker loudness does not influence NO_2 emission.

References

Clyne A. A., Thrush, B. A., and Wayne, R. P., 1964, "Kinetics of the Chemiluminescent Reaction between Nitric Oxide and Ozone," *Trans. Faraday Soc.*, Vol. 60, pp. 359~370.

Frenklach, M., Wang, H, Bowman, C. T., Hanson, R. K., Smith, G. P., Golden, D. M., Gardiner, W. C., and Lissianski, V., 1994, "An Optimized Kinetics Model for Natural Gas Combustion," *TwentyFifth Symposium (International) on Combustion*, Irvine, California, Work-In-progress Poster Session 3, Number 26.

Gaydon, A. G., 1974, *The Spectroscopy of Flames*, 2nd Ed., Chapman and Hall.

Jenkins, F. A. and White, H. E., 1976, *Fundamentals of Optics*, 4th Ed., MaGraw-Hill.

Kee, R. J., Rupley, F. M., and Miller, J. A., 1989, *Chemkin-II : A FORTRAN Chemical Kinetics Package for the Analysis of Gas Phase Chemical Kinetics*, Sandia National Laboratories, Sandia Report, SAND 89-8009B • UC-706.

Kee, R. J., Grcar, J. F., Smooke, M. D., and Miller, J. A., 1985, *A FORTRAN Program for Modeling Steady Laminar One-Dimensional Premixed Flames*, Sandia National Laboratories, Sandia Report, SAND 85-8240 • UC-401.

Lentini, L., and Puri, I. K., 1997, Radiation and NO_x Pathways in Nonpremixed Turbulent Flames, Submitted for Publication.

McManus, K. R., Poinsot, T., and Candel, S. M., 1993, "A Review of Active Control of Combustion Instabilities," *Prog. Energy Combust. Sci.*, Vol. 19, pp. 1~29.

Miller, J. A. and Bowman, C. T., 1989, "Mechanism and Modeling of Nitrogen Chemistry in Combustion," *Prog. Energy Combust. Sci.*, Vol. 15, pp. 287~338.

Pearse, R. W. B. and Gaydon, A. G., 1976, *The Identification of Molecular Spectra*, 4th Ed., Chapman and Hall, London.

Schimmer, H. and Vortmeyer, D., 1977, "Acoustical Oscillation in a Combustion System with a Flat Flame," *Combust. Flame*, Vol. 28, pp. 17~24.